Ion Transport through Gramicidin A. Water Structure and Functionality

M. Poxleitner, J. Seitz-Beywl, and K. Heinzinger

Max-Planck-Institut für Chemie (Otto-Hahn-Institut), Postfach 3060,
D-55020 Mainz, Bundesrepublik Deutschland

Z. Naturforsch. **48c**, 654–665 (1993); received December 28, 1992/April 5, 1993

Ion Transport, Gramicidin A, Molecular Dynamics, Functionality, Water Structure

Molecular Dynamics (MD) simulations were performed on a gramicidin A dimer model representing a transmembrane channel. Different from previous simulations the peptide was in contact with bulk water at both ends of the dimer to guarantee a realistic description of the hydration of the biomolecule. The flexible BJH model for water was employed in the simulations and the gramicidin-water, gramicidin-ion and ion-water potentials used are based on molecular orbital calculations. The water structure near the gramicidin was investigated first by a simulation without ions, while for the energy profiles of the ion transport through the channel a potassium or a sodium ion was added. These investigations provide a detailed and conclusive picture on a molecular level of the role of water in the ion transport through a gramicidin A channel and can explain the experimental results on the selectivity between alkali ions, their double or even triple occupancy, the exclusion or permeability of anions depending upon cation concentration and the consequences of differences in the ionic charge. The investigation demonstrate that the water molecules around the gramicidin behave as an integral part of the peptide and the functionality is the result of the whole complex biomolecule-water.

Introduction

The gramicidin A dimer is well known for its function as a channel for cation transport (see *e.g.* [1, 2]). It shows a number of interesting properties:

- Gramicidin A is selectively permeable for singly charged cations. The permeability coefficient increases with alkali ion size ([3] and references in [4]).
- Alkaline earth ions do not diffuse through the channel, but associate at its entrance [1].
- There is no transfer of anions through the channel except for high cation concentrations [5–7].
- Double occupancy of the channel is found for cations. The results even suggest occupancy numbers higher than two [8].

In spite of the huge amount of experimental work done on this system, the question of how all these reactions can occur is still hardly understood. Nearly all biochemical processes occur in an aqueous environment. Because of the polar and non-polar regions of a peptide, at least in the first layer the water structure is strongly influenced by the biomolecule. One can assume that this well defined hydration is decisive for the functionality of the peptide and can therefore not be neglected in the discussion. This active role of water is generally accepted, but the exact contribution of the water molecules to the functionality of the overall complex biomolecule-water is hardly understood [9, 10] because of difficulties in the experimental determination of the hydration structure of biomolecules. Computer simulations are a useful tool for an understanding of these experimental findings on a molecular level, as this system is too complicated for a treatment by analytical theory.

The big interest in gramicidin as a model for transmembrane transport is therefore reflected by the relatively large number of Monte Carlo (MC) and Molecular Dynamics (MD) simulations performed on this system. The models used in the simulations differ mainly in the simplifications concerning the amino acids, the allowed flexibility of the model and the peptide-water interactions. With a simple geometrical criterion the models can be divided in two groups, which are in short characterized by:

1) Simulations with an infinitely extended channel model:

This type of model was used by Skerra and Brickmann [11] as well as Roux and Karplus [12]. The influence of the channel entrance is completely neglected. Because of the periodic boundary conditions the lack of a water reservoir at both

Reprint requests to Dr. K. Heinzinger.

Verlag der Zeitschrift für Naturforschung,
D-72072 Tübingen
0939–5075/93/0700–0654 $ 01.30/0

entrances will (most probably) lead to an over or under occupation of the channel. The periodicity of the channel will furthermore result in an artificial preferential orientation of the hydrogen bonded water molecules.

2) Simulations of a gramicidin dimer (finite models):

In the investigations by Mackay *et al.* [13], Lee and Jordan [14] and Etchebest and Pullman [15] less than 24 water molecules were considered. Therefore the water molecules occupy essentially the channel interior and only some of them are found outside in the entrance region of the channel. The lack of a bulk phase does not lead to a realistic hydration sphere at the entrances. Because of the strong tendency to form hydrogen bonds this may affect the structure and orientation of the water molecules in the interior of the channel, too. In a more recent investigation by Chiu *et al.* [16] 25 water molecules were added at each end of the channel in form of a cap. Even in this case surface effects are expected to prevent bulk like properties. Fornili *et al.* [17] used about 80 water molecules in their simulations. To prevent water molecules from evaporation they introduced a cylindrical, repulsive wall with a radius of 5.5 Å at the entrances. The influence of this wall on the water structure at the entrance region has not been investigated.

In the MD-simulations reported here a large number of water molecules is employed which guarantees bulklike properties outside the channel and in this way provides a realistic hydration of the gramicidin. In order to describe the peptide hydration as realistic as possible we used a flexible water model which is able to react with internal distortion to the interaction with the biomolecule.

In the next chapter the model is described together with details of the simulation. The hydration of an ion-free gramicidin channel is investigated in a first simulation. By adding an ion to the system in various positions, all the above mentioned properties of gramicidin will be discussed.

Description of the Model and Details of the Simulation

The coordinates of the gramicidin dimer are taken from Urry [18]. The model (Fig. 1) consists of 552 atoms and is surrounded by 490 water molecules. Lennard-Jones (LJ) walls at ± 31.45 Å and ± 5.80 Å keep the water density constant and separate the two entrances of the channel. Periodic boundary conditions are used in the x- and y-directions.

In the Urry model the helix is left-handed. More recent investigations strongly indicate a right-handed one for gramicidin A [19, 20], however the earlier agreement of experimental data with left-handedness is still not resolved. The differences between the two kind of helices seem not to be of importance for the results reported here as in both cases three carbonyl groups extend into the solution due to the alternating D- and L-configurations of the amino acids.

An important point which has to be considered is that of the flexibility of the dimer and its possible influence on the results presented below. Certainly the lipid environment will constrain the channel and act as a modulator. In other simulations with flexible models [12, 21] the essential features of the backbone structure remained unchanged. There are also experimental hints that gramicidin A acts as a rigid channel [22]. The results presented below are of purely structural nature. The hydrogen bonding of the water molecules and the coordination of the ions are almost exclusively determined by the carbonyl groups. Therefore it is adequate to introduce flexibility for the carbonyl oxygens and keep the atoms of the backbone rigid.

The carbonyl oxygens have three vibrational degrees of freedom described by harmonic potentials, similar to the model of Skerra and Brickmann [11]. The modes represent the in-plane, ϑ, and out-of-plane, φ, torsional modes and the stretching mode, d, of the CO-bond. The variables of these modes are defined by a local coordinate system at each carbonyl group. The plane is given by the equilibrium position of the carbon and oxygen atom and the projection of the carbon on the channel axis. Therefore the equilibrium position has the coordinates $\vartheta = 0$, $\varphi = 0$, $d = d_o = 1.24$ Å. The potential energy function is defined as follows:

$$V(\varphi, \vartheta, d) = \frac{k_\varphi}{2}\varphi^2 + \frac{k_\vartheta}{2}\vartheta^2 + \frac{k_d}{2}(d - d_o)^2.$$

The constants are taken from the work of Dwivedi and Krimm [23], who performed force field

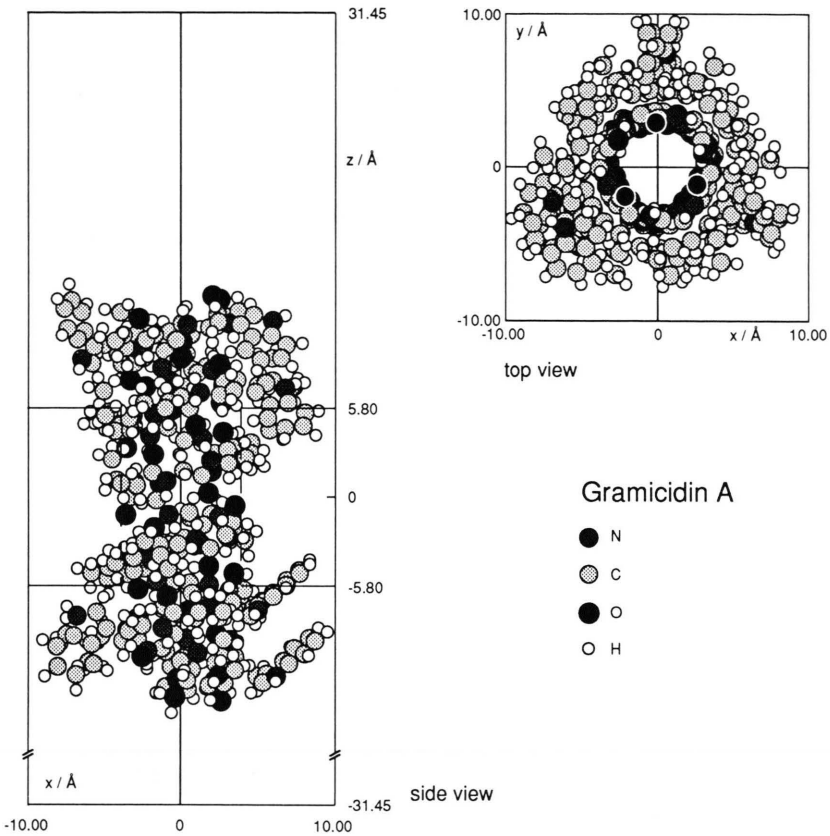

Fig. 1. Projection of all atoms of the gramicidin A dimer into the *xy*-plane (right) and the *xz*-plane (left) of the simulation box. The three outer most carbonyl oxygens on the left projection are marked by white circles.

calculations on a polyalanin molecule, with a surrounding similar to gramicidin. The values are 396 kJ mol^{-1} rad^{-1}, 753 kJ mol^{-1} rad^{-1} and $6040 \cdot 10^{-3}$ kJ/mol·Å^2 for k_φ, k_ϑ and k_d, respectively.

There is also an interaction assumed among the atoms of the carbonyl groups, which is described by a (12-6-1)-LJ-potential. The charge of the atoms is the same as in the case of the peptide-water interaction ($q_C = 0.45|e_o|$, $q_O = -0.44|e_o|$). The ϵ and σ for the C-C and O-O interaction are taken from Mackay *et al.* [13] and the Lorentz-Berthelot-rule was employed [24]. The parameters are given in Table I together with the LJ-parameters for the water-wall interactions.

The water-water interactions are described by the flexible BJH model [25] which has proved its usefulness in simulations of various aqueous systems [26, 27]. The gramicidin-water and gramicidin-ion potentials are taken from Fornili *et al.* [17] and Kim *et al.* [28, 29] derived from molecular orbital calculations and fitted to a (12-6-1)-LJ-function. The water-potassium and water-sodium potentials are derived from ab initio calculations. For the oxygen and hydrogen atoms the basis sets of Dunning [30] were employed, while for the sodium and potassium ions the MIDI*-basis sets proposed by Huzinaga *et al.* [31] were used. The functional form of the potentials and the parameters are presented in Table II.

Table I. Lennard-Jones parameters.

Interaction	σ [Å]	ϵ [kJ/mol^{-1}]
C–C	3.617	0.6191
O–O	2.860	0.9539
C–O	3.239	0.7684
$L_z/2$*	3.1	0.3168
z_m*	2.5	0.3168

* LJ-parameter for the water-wall interactions at $L_z/2 = \pm 31.45$ Å and at $z_m = \pm 5.80$ Å.

Table II. Potential functions potassium-water and sodium-water*.

$$V_{KO}(r) = -9.17 \times 10^2 \cdot r^{-1} - 3.77 \times 10^2 \cdot r^{-2} + 3.94 \times 10^5 \exp(-3.76 \cdot r)$$
$$V_{KH}(r) = 4.58 \times 10^2 \cdot r^{-1} + 1.55 \times 10^2 \cdot r^{-2} + 2.94 \times 10^4 \exp(-3.80 \cdot r)$$
$$V_{NaO}(r) = -9.17 \times 10^2 \cdot r^{-1} - 3.52 \times 10^2 \cdot r^{-2} + 3.55 \times 10^5 \exp(-4.30 \cdot r)$$
$$V_{NaH}(r) = 4.58 \times 10^2 \cdot r^{-1} + 1.52 \times 10^2 \cdot r^{-2} + 5.19 \times 10^4 \exp(-5.39 \cdot r)$$

* The energies are given in kJ/mol with the distance r in Å.

The shifted force method was employed for the short-range interactions while the two-dimensional Ewald-method [32] was used for the Coulomb-interactions. The time step length was 2.5×10^{-16} s. The simulation extended over 6.5 ps at an average temperature of 305 K for the ion-free simulation and 7.5 ps at an average temperature of 297 K and 300 K for the potassium ion at the entrance and in the interior, respectively.

The configuration of the ion-free simulation was created by placing a cube of bulk water from another simulation at each side of the channel. Additionally the channel interior was filled with eight water molecules. Then the simulation box was decreased in z-direction till a lamina with bulk density was achieved at both sides. After lengthy equilibrations, first at elevated temperature, data collection was started after total energy and temperature remained constant without rescaling.

Results and Discussion

Hydration of the gramicidin a dimer

Water structure in the entrance region

The good agreement of various structural, dynamical and thermodynamical properties of water in the region between $|z| = 19$ Å and 22.5 Å with those calculated from simulations of pure water demonstrates that not only the density but all other properties are very similar to those in the bulk. Obviously the influence of the gramicidin on water is a short ranging one, similar to what was found for LJ- and Pt-walls [27].

At both entrances of the gramicidin dimer the oxygen atoms of three carbonyl groups extend into the solution. Their strong interaction with the surrounding water molecules is demonstrated by the radial distribution function $g_{ij}(r)$ between these carbonyl oxygens and water as shown in Fig. 2. The distribution of the water molecules around the carbonyl oxygens is not spherically symmetric because of the excluded volume effect of the gramicidin atoms. Therefore, the $g_{ij}(r)$ have been calculated by taking into account the volume of the peptide as a function of the distance to the carbonyl oxygens. But the running integration numbers are based on the uncorrected RDFs in order to provide the correct number of neighbours. Only the water molecules with $|z| > 10$ Å are included in the RDFs, to distinguish this subsystem from that of the channel interior.

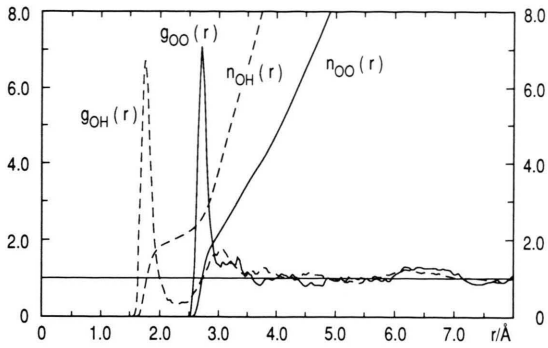

Fig. 2. Radial distribution functions and running integration numbers for carbonyl oxygen-water oxygen (full) and carbonyl oxygen-water hydrogen (dashed). For details of their calculation see text.

The carbonyl oxygen-water oxygen radial distribution function (RDF) has a peak at 2.7 Å, which is more pronounced and appears at shorter distances than the oxygen-oxygen distribution of pure water. It shows the strong interaction between the carbonyl groups and water. Thanki *et al.* [33] investigated the hydration of non-homologous proteins. The maximum of the distance distribution between carbonyl oxygen and water was found at 2.7 Å, in good agreement with this simulation. The number of nearest neighbours up to a distance of 3.1 Å is found to be 2.6 (Fig. 2). This coordination number is relatively high, considering the reduced space for water molecules in the entrance region.

The carbonyl oxygen-water hydrogen RDF is also given in Fig. 2. Again the first peak is much

stronger pronounced than the corresponding one in water. The integration up to the first minimum gives 2.1 hydrogen atoms which demonstrates that on the average two strongly directed hydrogen bonds are formed between water molecules and the carbonyl oxygens.

The orientation of the water molecules in the entrance region can be described by the distribution of cos φ, where φ is the angle between the dipole moment vector of a water molecule in the hydration shells of the three outer carbonyl groups and the unit vector parallel to the channel axis, for symmetry reasons pointing in the direction of increasing $|z|$-values. The result is given as the full line in Fig. 3. The pronounced peak near $\cos\varphi = -1$ indicates a strong preference for dipole vectors of water molecules directed parallel to the z-axis and towards the channel interior. There is a wide range of uniformly distributed orientations between $\cos\varphi \approx -0.7$ up to $\cos\varphi \approx 0.3$. There are practically no orientations found for angles $\varphi < 60°$. A more detailed investigation shows that the orientations with $\cos\varphi < -0.7$ mostly belong to water molecules which are positioned near the channel axis while the other water molecules hydrate the channel entrance laterally.

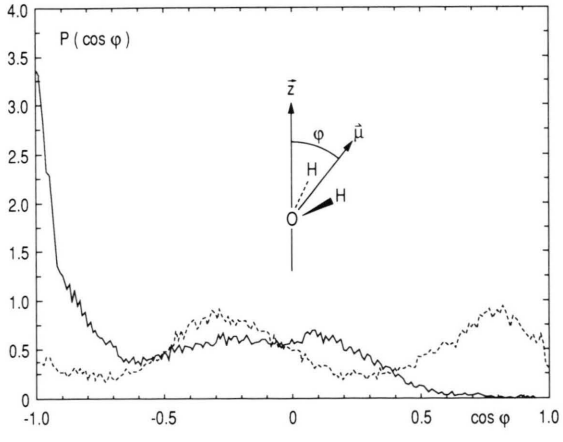

Fig. 3. Distributions of cos φ, where φ is the angle between the dipole moment vector of a water molecule at the channel entrance and the unit vector of the z-axis (pointing outward at both channel entrances). For water molecules with carbonyl oxygen-water oxygen distances $r < 3.1$ Å in the ion-free case (solid) and including those in the first hydration shell of the potassium ion (dashed).

Water structure in the interior of the channel

For the investigation of the structure of the water molecules in the channel interior those water molecules were included in this subsystem which are within the closed part of the helix ($|z| < 10$ Å). During the whole simulation the same 8 water molecules fullfilled this condition. Consequently a mean distance between the neighbouring oxygen atoms of 2.85 Å results, similar to that between first neighbours in a bulkwater phase.

A water molecule in the channel interior forms hydrogen bonds not only with its water neighbours but also with the carbonyl groups which are arranged as a helix around it. Therefore, it is of interest to consider the spacial orientations of these water molecules together with hydrogen bonding. In Fig. 4a one can recognize that two orientated chains of water molecules extend from both entrances of the channel into the interior. These water molecules form two different hydrogen bonds as donors. One bond which extends nearly parallel to the channel axis is formed with a neighbouring water molecule, while the second one – more perpendicular to the channel axis – is directed to the oxygen atoms of the carbonyl groups. A third hydrogen bond is formed by these molecules in the function of a proton acceptor from a water neighbour. These two chains are connected by a water molecule with a quite different orientation (marked by an arrow in Fig. 4a) where the dipole moment vector is nearly perpendicular to the channel axis. This molecule acts as a double acceptor for hydrogen bonding with its two water neighbours (double acceptor configuration), while two hydrogen bonds can be formed as a donor with the surrounding oxygen acceptors of the gramicidin.

The orientation found can be derived from the results mentioned above and the known properties of water. Water molecules have a high correlation of the dipole moment vector of next neighbours [34]. This has the consequence that the orientations of the water molecules at both channel entrances are continued from both sides into the channel interior as a linear and nearly parallel orientated chain. An energetical very unfavourable antiparallel orientation of two water neighbours in the interior causes the turn of one molecule, this means the forming of the double acceptor configuration. This leads to the conclusion that

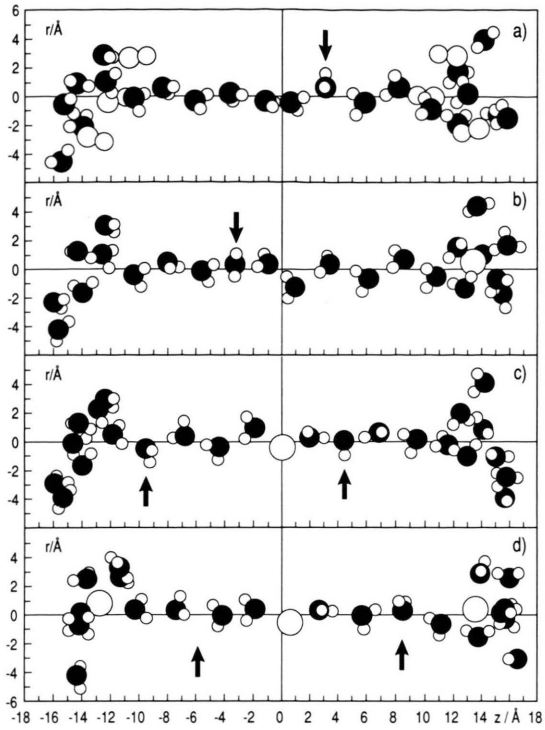

Fig. 4. Snapshots of the gramicidin-water and gramicidin-water-potassium ion simulations. Projection of the oxygen and hydrogen atoms of the water molecules at the channel entrance and in the channel interior onto a *zr*-plane. *r* is the distance from the *z*-axis. a) The carbonyl groups at the channel entrances are shown additionally (Fig. 1). b) The cation is placed in the entrance region. c) The cation is placed in the channel center. d) One cation is placed in each entrance region and one cation in the channel center. In all figures the arrows mark water molecules which act as a double acceptor for hydrogen bonds with their water neighbours while the left arrow in d) marks a break in the hydrogen bonded chain of the water molecules.

the described structure in the channel interior is the result, both of the interaction of the water molecules with their water neighbours and the peptide and the hydration structure at the channel entrances.

The discribed structure of two antiparallel water chains, connected by a double acceptor configuration guarantees that a maximum amount of hydrogen bonds can be formed. The position of the double acceptor configuration in the channel is arbitrary for the mentioned function. During the whole simulation time the same molecule remained in that configuration. Roux and Karplus [12], who found an exclusively parallel orientation of the water molecules in their one dimensional periodic model, observed only one turn of the whole configuration during a simulation time of 250 ps.

The simulation of Fornili *et al.* [17] with about 80 water molecules in the entrance regions resulted in two antiparallel water chains in the channel, as in this work.

Contrary to our work, Chiu *et al.* [21] even found a water molecule in the channel in a double donor instead of a double acceptor configuration. The number of possible hydrogen bonds was therefore reduced. Jordan [35] described configurations with hydrogen atoms pointing out of the channel at both ends as "typical" for the arrangement of the water molecules. Mackay *et al.* [13] described one parallel water chain in the whole channel. This structure means two different entrances, in contradiction to the symmetry of the channel.

Such configurations seem to be possible only because of the lack of a sufficient amount of water molecules at the channel entrances, so that an induced orientation of the water molecules from the channel ends to the interior cannot occur. The cases above show that even for finite simulation models different water molecule configurations in the channel interior are described in the literature. Either all dipole moment vectors point in the same direction or two different antiparallel orientations can be found. Of course, a larger number of water molecules in the model means a more realistic description of the natural conditions where a hydration sphere and a bulk solution exist. Furthermore it is our intention to show that all the described water configurations can be understood by considering the details of the simulation models used.

Cation versus anion selectivity

Evidently the orientation of the water molecules hydrating the channel entrance is favourable for the approach of a cation along the *z*-axis or even laterally (capture region). The ion can be fixed to the hydration sphere without a reorientation of the water molecules in the whole entrance region or even in the channel interior. Such an ion access may increase the probability for ions to enter the channel, because they are kept near the channel and the rate for a diffusion back into the solution is reduced [36].

This water molecule orientation, of course, prevents anions from approaching and consequently entering the channel although the structure of the peptide should not be responsible for an exclusion of anions (see *e.g.* the discussion in [37]). A possible deviation from this conclusion will be discussed below.

Gramicidin A and ions

Energy profiles for cations

In order to obtain a profile of the minimum potential energy of cations, which characterizes the reaction coordinate through the channel, further simulations with one sodium or one potassium ion in addition to the water molecules were performed for different z-values. The cations were fixed in the xy-plane while no constraint acted on the water molecules or the flexible gramicidin atoms. After reaching a potential energy minimum the simulation was continued with the corresponding configuration for at least 2000 time steps. If a deeper minimum developed, this procedure was repeated until no further decrease in energy occurred. The minimum energy profile permits to specify points of the reaction coordinate which are of specific interest for a further investigation. This is a simplification, as even with the largest computers available the movement of an ion to and through the gramicidin channel cannot be followed.

The results are shown in Fig. 5. For both ions the energy minima along the reaction coordinate are found between the two outer carbonyl oxygens at $|z| \approx 13$ Å. For both ions an increase of the energy at the channel entrance can be recognized. The maximum of the barrier appears at $|z| \approx 10$ Å for both cations and is larger for the sodium ion in agreement with the known selectivity sequence. Energy variations towards the middle of the channel seem not to be statistically significant because of the regular structure of the peptide backbone and therefore of the carbonyl groups [38].

As the minimum of the reaction path close to the channel mouth is of special interest, we performed a simulation with a potassium ion there. During the whole simulation time the potassium ion remained in the open part of the channel helix at $|z| = (13.2 \pm 0.3)$ Å which can be considered as the assoziation site of the channel for a cation. The

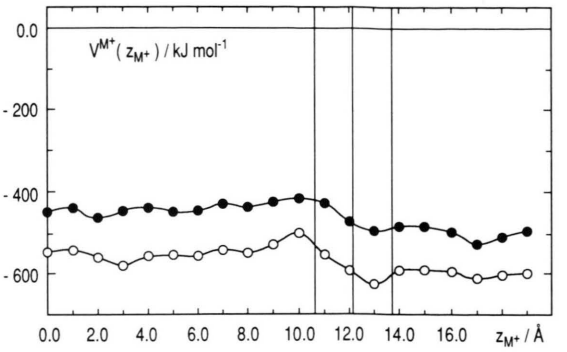

Fig. 5. Minimum energy of a cation M^+ (potassium (●) or sodium (○)) as a function of its z-coordinate (see text for a more detailed description). The perpendicular lines mark the z-coordinates of the outer most carbonyl oxygens.

overall position of the binding site is in agreement with the minimum of the energy profile of Fig. 5.

Electrochemical and spectroscopic investigations suggest a binding site in the region between 10 Å and 11 Å. It was calculated with the assumption that Eyring's rate theory can be used here. Whether this procedure is correct or not is still under discussion [1, 39–41]. Koeppe *et al.* [42] report X-ray experiments on gramicidin A and give a binding site of about 11 Å. But it is not sure whether the investigated structure is the same as in the case of a membrane-bound channel [43] because under those conditions gramicidin forms probably antiparallel double helices and no head-to-head dimers [44]. Urry *et al.* [45] concluded from NMR measurements that two symmetric binding sites for monovalent cations are localized between the Trp 11 and Trp 13 carbonyl groups of each monomere. Furthermore Olah *et al.* [46] give binding sites for Tl^+ at about 9.6 Å and for Ba^{2+} at about 13.0 Å, whereby the location of the Tl^+-binding site is surprising because it was generally thought that monovalent cations bind at the first turn of the helix [47, 48]. Finkelstein and Andersen [49] found experimentally that gramicidin shows water permeability even with a sodium ion at the channel entrance. They concluded, consistent with the simulation results, the existence of a binding site in the open region of the helix. Fig. 4b gives a snapshot from the simulation which is able to illustrate the described situation. The potassium ion position at the channel entrance does not block the

channel for water molecules. This point will be investigated in more detail below.

Coordination of the potassium ion at the association site

The next step in the investigation of ion selectivity is the calculation of the ion-oxygen coordination in the entrance region.

The normalized potassium ion-peptide oxygen distance distribution is shown as a full line in Fig. 6. In the Urry model the ethanolamine tail has the energetically favourable staggered conformation. Because of the position at the channel entrance (see Fig. 1), its oxygen atom can also coordinate the potassium ion and is therefore included here. There are four peaks up to the first pronounced minimum at 4.7 Å, which are connected with the three outer carbonyl oxygens and the ethanolamine oxygen. Because of the movement of the cation at the association site the four peaks are not well defined but overlap. Together they define the solvation sphere of the cation by the peptide. The total number of peptide oxygens, $n_{KO}(d)$ up to the distance of d = 4.7 Å, is 4. The distribution function shows two pronounced peaks at larger distances, each of them caused by two carbonyl oxygens in the channel interior. They are well separated as the distances between the potassium ion and these oxygen atoms are not changed much by the motion of the cation in the entrance region.

The coordination of the water molecules to the K^+ in the entrance region is described by the K^+-oxygen RDF, calculated as explained above. It is presented in Fig. 7. In Table III the characteristic

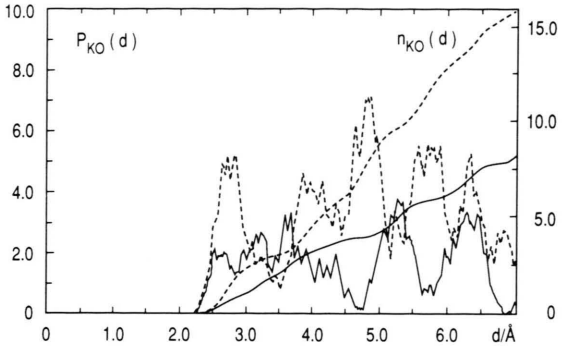

Fig. 6. Distribution $P_{KO}(d)$ of the distances between the potassium ion and the oxygens of gramicidin A. The full line refers to the simulation with a potassium ion at the channel entrance (including the ethanolamine oxygen), while the dashed line gives the coordination by carbonyl oxygens when the cation is in the middle of one monomer. The integration numbers $n_{KO}(d)$ are given on the right axis.

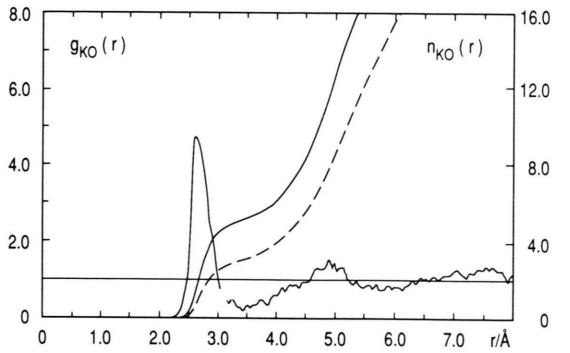

Fig. 7. Radial distribution functions for potassium ion-water oxygen $g_{KO}(r)$. The full line gives the running integration number for all the atoms, while the dashed one considers only those which fullfill the condition $z_O > z_{K^+}$.

Table III. Characteristic values* of the potassium-water pair distribution functions.

i j		R_1	r_{M1}	$g(r_{M1})$	r_{m1}	$g(r_{m1})$	r_{M2}	$g(r_{M2})$	$n(r_{m1})$
K O	(e)	2.5	2.7	4.7	3.5	0.3	4.9	1.4	5.2
	(b)	2.48	2.69	5.37	3.68	0.49	5.08	1.49	7.5
K H	(e)	2.9	3.3	2.3	4.2	0.6	5.4	1.2	14.1
	(b)	3.01	3.33	2.72	4.24	0.56	5.67	1.36	18.4

* R_k, r_{Mk} and r_{mk} are the distances in Å where $g_{ij}(r)$ first becomes 1 or has its k-th maximum or minimum, respectively. n is the number of next neighbours, defined as the spacial integral up to the first minimum. (e) and (b) give the characteristic values of the pair distribution functions for K^+ in the entrance region and the bulk solution, respectively.

values both of the K^+-oxygen and K^+-hydrogen RDF are compared with those of a 2.2 molal KCl bulk solution, for the simulation of which the same water-water and potassium-water potentials were employed. The comparison shows only small deviations for the distances of the characteristic points. Only the heights of the peaks show differences because of the different surroundings – peptide or bulk. The number of nearest neighbours of K^+ in the entrance region is 5.2. Compared with the bulk solution this means that the hydration number is reduced by 2.3 because of the excluded volume effect of the gramicidin. Thus the potassium ion at the channel entrance is coordinated by 4 peptide and 5.2 water oxygens. This high solvation number explains the position of the binding site in the open part of the helix, where such a high coordination is solely possible.

It is interesting to distinguish whether a water molecule in the first shell of K^+ is positioned towards the bulk $z_O > z_{K^+}$ or in the direction of the channel interior $z_O < z_{K^+}$. The dashed line in Fig. 7 shows the number of water molecules with $z_O > z_{K^+}$ as a function of distance. Up to the first minimum 3.2 neighbours are found. This means that two water molecules are between the ion and the one-dimensional water structure in the channel interior. The water structure is therefore not interrupted from the channel interior to the bulk, in agreement with the above mentioned water permeability if a cation is bound at the channel.

In Fig. 3 the distribution of the orientation of those water molecules which hydrate the ion occupied channel entrance – the carbonyl oxygens or the potassium ion – is shown as a dashed line. Different from the ion-free case a maximum appears at $\cos\varphi = 0.8$. Obviously it marks the orientation of dipole moment vectors of those water molecules which are bound to the cation and have $z_O > z_{K^+}$. Because of the interaction of these water molecules in the hydration sphere of the cation among each other and with the carbonyl groups in the neighbourhood, it can be understood that they are not preferentially parallel to the z-axis. Anyway, one has to keep in mind that the z-axis is not the symmetry axis of the channel entrance, but only of the channel interior. The number of water molecules with orientations antiparallel to the z-axis ($\cos\varphi = -1$) is strongly reduced, as the position close to the channel entrance is now occupied by the cation. A second maximum is found at $\cos\varphi \approx -0.3$. This reflects, as in the ion-free case, the orientations of the dipole moment vectors of those water molecules which hydrate the channel laterally.

Coordination of the potassium ion in the channel interior

In order to understand the selectivity it is important to know how the coordination of K^+ in the channel interior differs from that at the association site. For this purpose a simulation with a potassium ion at $z \approx 4$ Å (Fig. 1, side view) was performed. The distribution of the distances between the potassium ion and all the peptide oxygens is shown as a dashed line in Fig. 6. A clear peak can be seen at $d \approx 2.7$ Å in agreement with the typical potassium-oxygen first neighbour distance. The integration up to the well-defined minimum at 3.5 Å leads to a coordination number of 3. Three further oxygens form a second peak up to 4.5 Å. The peaks at larger distances reflect the remaining carbonyl oxygens, which become less at distances beyond about 6 Å because of the limited channel length and asymmetric position of K^+ in the channel interior. The channel diameter permits only two water molecules as nearest neighbours to the K^+ in the interior. Their cation-oxygen distribution is shown in Fig. 8. The distribution is rather narrow and the maximum appears at a distance smaller than in the bulk, indicating a strong cation hydration.

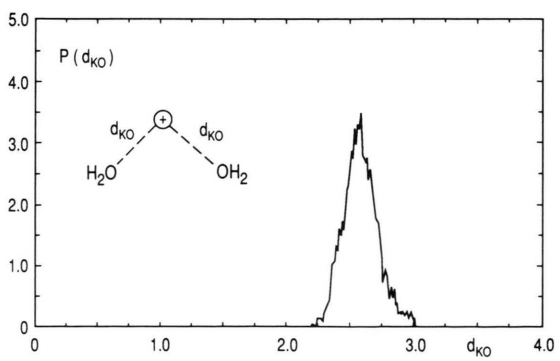

Fig. 8. Distribution of the distances d_{KO} between the potassium ion in the middle of one monomer and the oxygen atoms of its two closest water neighbours.

Cation selectivity

The permeability coefficients of singly charged cations as deduced from experiment show the following sequence:

$$P_{Li^+} < P_{Na^+} < P_{K^+} < P_{Rb^+} \approx P_{Cs^+} < P_{H^+}.$$

The differences between the larger alkali ions are rather small. Compared with sodium, the coefficients for potassium and cesium are larger by 47% and 55% [47], respectively.

In the case of gramicidin there is still a discussion about the question whether the entry into or the diffusion through the channel is the rate determining step for the selectivity. The energy profiles in Fig. 5 demonstrate that for the diffusion of a cation in the interior of the gramicidin channel no big changes in the energy occur as the carbonyl groups form a regular structure, which continues over the junction of the monomers [38]. This is different in the entrance region. In going from the bulk to the association site the hydration number of the potassium ion is reduced from 7.5 to 5.2, but the cation is solvated by 4 oxygens of the peptide. The entering of the channel is connected with a further loss of 3.2 water molecules, because in the channel interior the cation is only hydrated by two water molecules. The solvation number of the peptide oxygen is increased by about two. This means that during the first partial dehydration (association step), the potential energy decreases, while the second partial dehydration (entering the channel) is connected with an increase in potential energy. This two step reaction may be written in the following way:

$$K^+(H_2O)_{7.5} + GA \overset{-2.3\,H_2O}{\rightleftharpoons} GA(K^+)_{ass}(H_2O)_{5.2} \overset{-3.2\,H_2O}{\rightleftharpoons} GA(K^+)_{int}(H_2O)_2.$$

It can be concluded from these results that neither the diffusion through the channel, nor the association step is rate determining, but the entering into the channel. We already mentioned that the energy barriers at the channel entrance reproduce the selectivity sequence between sodium and potassium correctly. For a better understanding of the selectivity it is important to know whether the increase of the potential energy results mainly from the interactions of the cation with gramicidin or with water. The number of nearest neighbour peptide oxygens is larger by about two in the interior than at the channel entrance (Fig. 6), and generally the running integration number gives higher values for all distances. This means a better coordination of the cation by the peptide and a lower cation-peptide energy in the channel interior compared with the state when the ion is bound at the entrance. This is in accordance with the energy profiles of sodium and potassium along the z-coordinate calculated by Kim and Clementi [38]. For both cations they found in the region 10 Å $< z <$ 13 Å, nearly constant energy values for the peptide contribution. Then, these energy values decrease and reach nearly constant values in the interior of the channel. The profile of the cation-water interaction is different. In the above mentioned interval the profiles increase. This means that the cation suffers – caused by a partial dehydration – a loss of binding energy concerning water. In the channel interior the profile is nearly constant, too.

Consequently, the stripping of water molecules during the entrance step into the channel causes the increase of the energy in region 10 Å $< z <$ 13 Å shown in Fig. 5. The barrier for this step is therefore determined by the alkali ion-water interaction energies. The depth of these potential functions correlate with the above mentioned sequence of the alkali ion selectivity of gramicidin A.

Analogously, the experimentally known properties of the alkaline earth (divalent) ions in contact with gramicidin can be understood, too. In the literature [1] an association of alkaline earth ions at the channel is described, but a diffusion through the channel cannot be found. Furthermore, a dynamical equilibrium between the alkaline earth ions in solution and associated at the channel entrance was detected. These results are in agreement with the discussion above that not the association but the next step, the entrance into the channel, is rate determining. The binding energies of the alkaline earth ions to a water molecule are significantly larger than for the alkali metal ions because of the double charge. Therefore a further dehydration necessary for entering the channel is energetically not possible.

Multiple occupancy by cations and anion permeability

Conductivity measurements and other investigations indicate [8, 50] that the channel can be oc-

cupied by two alkali ions. It is assumed that these cations are positioned at the two channel entrances. A so-called "knock on reaction" [51], whereby one of the ions enters at the already occupied side, is excluded for electrostatic reasons [43]. A doubly occupied channel is blocked for ion transfer.

Double occupancy is in complete agreement with the results of this work. One can see from Fig. 4b that the hydration of the entrance at the ion-free side (left) of the ion-occupied gramicidin is in principle the same as shown in Fig. 4a at both entrances. This is due to the existence of a water molecule in double acceptor configuration (arrow in Fig. 4b). The conditions for the approach and the binding of a second cation are therefore the same as discussed above for ion-free case.

Based on experiments, Eisenman *et al.* [8] assumed the existence of gramicidin channels, which are occupied by three or even more cations. It is imagined that in such a case one cation is found in the channel interior while the other two cations are located at the entrances [43]. Again this result can be explained by the simulation. Fig. 4c shows a snapshot from a simulation with a cation in the middle of the channel (junction of the monomers). The orientations of the dipole moment vectors of the water molecules at the channel entrances can remain essentially the same as in the ion-free case, because two water molecules in double acceptor configuration exist. The conditions for the association of two further cations at the entrances are therefore fullfilled as discussed above. To check this we performed a simulation with three potassium ions – one placed at each channel entrance and one in the middle of the gramicidin. A snapshot of that investigation is shown in Fig. 4d. Here one water molecule acts as a double acceptor (right arrow) in one half of the channel. There is a clear hydrogen bonded chain of water molecules between the potassium ion at the right association site and that in the interior of the channel. Because of the fixed positions of the association sites at the entrances, and because there is not sufficient space for another water molecule, a break in the hydrogen bonded chain occurs in the second half of the channel (left arrow). The direction of the dipole moments is there determined by the strong hydration of the two cations and the interaction between the water molecules and the channel interior. This leads to the gap between two neighbouring water molecules which point with their dipole moments in opposite directions. This arrangement of three solvated cations in the channel which are at least partly connected by water molecules can therefore explain the stability of the suggested triple occupancy of gramicidin in spite of the high number of positive charges in a distance range of about 13 Å.

While no anion permeability can be measured under normal experimental conditions, Eisenman *et al.* [8] found at high thallium concentrations – when both channel entrances are occupied by thallium ions caused by the high affinity of thallium towards gramicidin – a permeability of acetate and chloride ions which reaches 10% of the value for the thallium ions. The simulation with a potassium ion associated at the channel entrance is appropriate to discuss this phenomenon because potassium and thallium are similar in a number of properties.

Different from the ion-free case, the cation at the channel entrance reorientates the water molecules in the outer sphere of the hydration shell (Fig. 3 and Fig. 4b). Their dipole moment vectors point preferentially towards the bulk. This orientation of the water molecules should permit anions to approach the channel and enter it together with the cation. At this stage of the investigation it cannot be decided on the basis of the simulations whether the diffusion of the Tl^+/Cl^--complex occurs as a contact ion pair or a solvent separated one. Electrostatic calculations suggest a contact ion pair [43]. This question is currently investigated in our laboratory.

Acknowledgements

A grant of computer time from the Höchstleistungsrechenzentrum für Wissenschaft und Forschung der Kernforschungsanlage Jülich and financial support by Deutsche Forschungsgemeinschaft is gratefully acknowledged.

[1] D. W. Urry, in: Topics in Current Chemistry, **Vol. 128** (F. L. Boschke, ed.), Springer Verlag, Berlin, Heidelberg, New York 1985.
[2] V. Ivanov and S. V. Sychev, in: Biopolymer Complexes (G. Snatzke and W. Bartman, eds.), Wiley and Sons Interscience, New York 1982.
[3] V. B. Myers and D. A. Haydon, Biochim. Biophys. Acta **274,** 313 (1972).
[4] A. Skerra and J. Brickmann, Biophys. J. **51,** 977 (1987).
[5] J. F. Hinton and R. E. II. Koeppe, Metal Ions in Biological Systems **19,** 173 (1985).
[6] G. Eisenman, J. Sandblom, and E. Neher, Biophys. J. **22,** 307 (1978).
[7] G. Eisenman, J. Sandblom, and E. Neher, in: Metal-Ligand Interactions in Organic Chemistry and Biochemistry, Part 2 (B. Pullman and N. Goldblum, eds.), Reidel, Dordrecht, Holland 1977.
[8] G. Eisenman, J. Sandblom, and E. Neher, in: Membrane Transport Processes, **Vol. 2** (D. C. Tosteson, Yu. A. Ovchinnikov, and R. Latorre, eds.), Raven Press, New York 1978.
[9] J. L. Finney and F. J. Savage, in: The Chemical Physics of Solvation, Part C (R. R. Dogonadze, ed.), Elsevier Science Publishers, Amsterdam, Oxford, New York, Tokyo 1988.
[10] J. L. Finney, in: Water – A Comprehensive Treatise (F. Franks, ed.), Plenum Press, New York 1979.
[11] A. Skerra and J. Brickmann, Biophys. J. **51,** 969 (1987).
[12] B. Roux and M. Karplus, Biophys. J. **59,** 961 (1991).
[13] D. H. J. Mackay, P. H. Berens, K. R. Wilson, and A. T. Hagler, Biophys. J. **46,** 229 (1984).
[14] W. K. Lee and P. C. Jordan, Biophys. J. **46,** 805 (1984).
[15] C. Etchebest and A. Pullman, J. Biomol. Structure and Dynamics **5,** 1111 (1988).
[16] S.-W. Chiu, E. Jakobson, S. Subramaniam, and J. A. McCammon, Biophys. J. **60,** 273 (1991).
[17] S. L. Fornili, D. P. Vercauteren, and E. Clementi, Biochim. Biophys. Acta **771,** 151 (1984).
[18] D. W. Urry, Proc. Natl. Acad. Sci. U.S.A. **68,** 672 (1971).
[19] L. K. Nicholson and T. A. Cross, Biochemistry **28,** 9379 (1989).
[20] O. S. Andersen, L. L. Providence, and R. E. Koeppe, Biophys. J. **57 a** (Abstr.) (1990).
[21] S.-W. Chiu, S. Subramaniam, E. Jakobson, and J. A. McCammon, Biophys. J. **56,** 253 (1989).
[22] S. H. Heinemann and F. J. Sigworth, Biophys. J. **57,** 499 (1990).
[23] A. M. Dwivedi and S. Krimm, Biopolymers **23,** 923 (1984).
[24] M. P. Allen and D. J. Tildesley, Computer Simulation on Liquids, Clarendon Press, Oxford 1987.
[25] P. Bopp, G. Jansco, and K. Heinzinger, Chem. Phys. Lett. **98,** 129 (1983).
[26] K. Heinzinger, in: Computer Modelling of Fluids, Polymers and Solids (C. R. A. Catlow, S. C. Parker, and M. P. Allen, eds.), Kluwer Academic Publishers, Dordrecht 1990.
[27] J. Seitz-Beywl, M. Poxleitner, and K. Heinzinger, Z. Naturforsch. **46 a,** 876 (1990).
[28] K. S. Kim, D. P. Vercauteren, M. Welti, S. L. Fornili, and E. Clementi, IBM Technical Report Pok.-42 (1984).
[29] K. S. Kim, D. P. Vercauteren, M. Welti, S. Chin, and E. Clementi, Biophys. J. **47,** 327 (1985).
[30] T. H. Dunning, J. Chem. Phys. **53,** 2823 (1970).
[31] S. Huzinaga, J. Andzelm, M. Klobukowski, E. Radzio-Andzelm, Y. Sakai, and H. Tatewaki, Gaussian Basis Sets for Molecular Calculations, Elsevier Science Publishers, Amsterdam, Oxford, New York, Tokyo 1984.
[32] D. M. Heyes, M. Barber, and J. H. R. Clarke, J. Chem. Soc., Faraday Trans. II **73,** 1485 (1977).
[33] N. Thanki, J. M. Thornton, J. M. Goodfellow, J. Mol. Biol. **202,** 637 (1988).
[34] Gy. I. Szász, K. Heinzinger, and W. O. Riede, Z. Naturforsch. **36 a,** 1067 (1981).
[35] P. C. Jordan, J. Phys. Chem. **91,** 6582 (1987).
[36] J. Sandblom, in: International Symposium Adelaide, Australia (A. H. Bretag, ed.), Adelaide 1983.
[37] D. G. Levitt, in: The Chemical Physics of Solvation, Part C (R. R. Dogonadze, ed.), Elsevier Science Publishers, Amsterdam, Oxford, New York, Tokyo 1988.
[38] K. S. Kim and E. Clementi, J. Am. Chem. Soc. **107,** 5504 (1985).
[39] G. Eisenman and J. P. Sandblom, Biophys. J. **45,** 88 (1984).
[40] D. G. Levitt, Biophys. J. **37,** 575 (1982).
[41] P. Läuger, W. Stephan, and E. Frehland, Biochim. Biophys. Acta **602,** 167 (1980).
[42] R. E. II. Koeppe, J. M. Berg, K. O. Hodgson, and L. Stryer, Nature **279,** 723 (1979).
[43] H. Monoi, J. Theor. Biol. **102,** 69 (1983).
[44] B. A. Wallace, Biophys. J. **49,** 295 (1986).
[45] D. W. Urry, in: The Enzymes of Biological Membranes, **Vol. 1** (A. N. Martonosi, ed.), Plenum Publishing Corporation, New York 1985.
[46] G. A. Olah, H. W. Huang, W. Liu, and Y. Wu, J. Mol. Biol. **218,** 847 (1991).
[47] S. B. Hladky and D. A. Haydon, Curr. Top. Membr. Transp. **21,** 327 (1984).
[48] P. C. Jordan, in: Current Topics in Membranes and Transport, **Vol. 33** (W. S. Agnew *et al.,* eds.), Academic Press, New York 1988.
[49] A. Finkelstein and O. S. Andersen, J. Membr. Biol. **59,** 155 (1981).
[50] S. B. Hladky, Curr. Top. Membr. Transp. **33,** 15 (1988).
[51] S. B. Hladky, B. W. Urban, and D. A. Haydon, in: Membrane Transport Processes, **Vol. 3** (C. F. Stevens and R. W. Tsien, eds.), Raven Press, New York 1979.